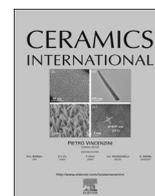




Contents lists available at ScienceDirect

Ceramics International

journal homepage: www.elsevier.com/locate/ceramint

Refractories containing fused and sintered alumina aggregates: Investigations on processing, particle size distribution and particle morphology

Stefan Schafföner^{a,*}, Christin Dietze^a, Steffen Möhmel^b, Jens Fruhstorfer^a, Christos G. Aneziris^a

^a Institute of Ceramic, Glass and Construction Materials, TU Bergakademie Freiberg, Agricolastrasse 17, 09599 Freiberg, Germany

^b Center for Abrasives and Refractories Research and Development GmbH, Seebacher Allee 64, 9524 Villach, Austria

ARTICLE INFO

Keywords:

C. Thermal shock resistance
C. Creep
E. Refractories
Particle size distribution

ABSTRACT

The present study investigated pressed high-purity alumina refractories containing either white fused or tabular (sintered) alumina aggregates under comparable conditions. Using factorial experiments especially the effects of the pressing pressure, the particle size distribution model and the particle morphology were evaluated. White fused alumina exhibited a higher refractoriness under load as well as a lower total compression and creep rate in creep in compression experiments. However, tabular alumina had a higher cold crushing strength and Young's modulus before and after thermal shock. Yet, no significant effect regarding the relative loss of the Young's modulus due to thermal shock was determined. Generally, a higher pressing pressure reduced the apparent porosity and increased the cold crushing strength, the Young's modulus and the refractoriness under load. The batches according to a recently suggested modified Andreasen particle size distribution model contained a considerably higher amount of the coarsest particle fraction, while the medium particle size fractions were reduced. Surprisingly, for both alumina raw materials the modified Andreasen model resulted in a virtually identical apparent density and a slightly lower apparent porosity compared to the conventional Andreasen model. Furthermore, the thermomechanical properties were essentially unaffected, while the cold crushing strength and the Young's modulus were somewhat lower. For both raw materials the addition of blocky coarse grain fractions yielded a lower apparent porosity and higher apparent density compared to angular grains due to improved particle packing. Remarkably, the creep in compression and the creep rate were reduced as well. Consequently, the modified Andreasen model together with a designed particle morphology might allow the fabrication of shaped alumina products with a much higher content of coarse grained particles resulting in at least similar or even improved physical, mechanical and thermomechanical properties irrespective of the used alumina raw material.

1. Introduction

Alumina is one of the most widely used raw materials for refractory applications due to its high refractoriness and due to its high erosion and corrosion resistance under many conditions [1–6]. Alumina raw materials are used in various kinds of refractory products including monolithics and shaped products as well as for the production of calcium aluminate cements [7–12].

In general three synthetic corundum raw materials are produced for refractory applications comprising tabular alumina (TA), white fused alumina (WFA) and brown fused alumina (BFA) [2,5,13].

The common primary material for tabular alumina and white fused alumina is calcined alumina of high purity from the Bayer process,

while bauxite ores are used for the production of brown fused alumina [2,13,14]. In the Bayer process aluminum hydroxide precipitates after the extraction of bauxite using sodium hydroxide, while some of the sodium remains in the aluminum hydroxide as an impurity. For a complete conversion to $\alpha - \text{Al}_2\text{O}_3$, the precipitated and washed aluminum hydroxide is then fired in rotary kilns at temperatures above 1200 °C resulting in the calcined alumina [15].

Tabular alumina is produced during a sintering process of at least 1800 °C using shaft kilns [16]. White fused alumina, on the other hand, results from the fusion of calcined alumina in an electric arc furnace. After the sintering and electrofusion process, respectively, the material is crushed, milled, and sieved in order to obtain the necessary grain sizes of the finally packaged alumina raw materials [2].

* Corresponding author.

E-mail address: schaffoener@gmail.com (S. Schafföner).

<http://dx.doi.org/10.1016/j.ceramint.2016.12.067>

Received 28 October 2016; Received in revised form 5 December 2016; Accepted 12 December 2016
0272-8842/ © 2016 Elsevier Ltd and Techna Group S.r.l. All rights reserved.

Tabular alumina consists of elongated, tablet-shaped crystallites with a size of 0.05–1 mm and a significant proportion of closed pores of about 5 vol%. The closed pores are evenly distributed and have usually a pore diameter of less than 10 μm while an average pore diameter of 0.71 μm was reported [6,16,17]. The crystallites of white fused alumina are generally much larger than the ones of tabular alumina and have a closed porosity of less than 1 vol% [17]. Compared to tabular alumina, the average pore size in white fused alumina is considerably larger (31–47 μm) and the pores are less evenly distributed, whereas the open porosity of white fused alumina was described as somewhat higher than the one of tabular alumina [16–19]. Meanwhile the total porosity, i.e. the sum of open and closed porosity, for white fused alumina was reported as slightly lower compared to tabular alumina [17].

The main impurity in tabular alumina and white fused alumina is sodium from the alumina extraction in the Bayer process. The sodium impurities cause the formation of $\beta - \text{Al}_2\text{O}_3$, which has a significant lower hardness than $\alpha - \text{Al}_2\text{O}_3$ and also decreases the refractoriness at higher temperatures due to low melting phases in the pseudobinary phase diagram $\text{Na}_2\text{O}-\text{Al}_2\text{O}_3$ [20]. Generally the total sodium content of the final alumina raw material is determined by the sodium impurities of the used primary calcinated alumina. Nevertheless, some studies reported a slightly higher level and variance of the sodium impurities in the fine grained particle fractions of white fused alumina compared to tabular alumina [17–19].

Nonetheless, the sodium impurities are in general more concentrated at grain boundaries. Due to the smaller crystallite size of tabular alumina, the relative amount of grain boundaries and thus the sodium impurities are evenly distributed in all grain size fractions. By contrast, because of the larger crystallite size in white fused alumina, it contains less grain boundaries. During crushing and milling to produce finer grain size fractions, white fused alumina is preferably comminuted along the grain boundaries rich in $\beta - \text{Al}_2\text{O}_3$, which have a lower hardness. Thus, $\beta - \text{Al}_2\text{O}_3$ and the sodium impurities tend to be accumulated in the finer grain size fractions of white fused alumina [16,17].

In general, tabular alumina grains have a lower apparent density than white fused alumina grains of comparable size, which can be attributed to the larger amount of closed pores in tabular alumina and is a general trend comparing sintered with fused refractory raw materials [16,21,22]. Even so, some studies reported a higher apparent density of tabular alumina compared to white fused alumina [18,19]. For both raw materials an increasing apparent density can be observed with a smaller grain size, which is caused by the elimination of closed pores by crushing and milling to produce smaller grain size fractions [21,23,24].

The high amount of closed pores in tabular alumina is generally believed to result in an improved thermal shock resistance compared to refractories of white fused alumina [2,14]. Furthermore, Bertrand et al. [25] determined higher strength values and higher Weibull moduli for tabular alumina compared to white fused alumina grains.

However, due to their specific processing, commercial tabular and white fused alumina raw materials normally have considerably different particle morphologies and particle size distributions [16]. Yet, these factors have a significant influence on the resulting properties of refractory products [16,23,26,27]. Consequently, it still remains to some extent unclear how refractory products of tabular and white fused alumina perform without confounding factors such as processing, particle morphology and particle size distribution.

Consequently, the aim of the present study is to study pressed high purity alumina refractories made of either tabular (sintered) or white fused alumina raw materials under comparable conditions. For that purpose the pressing pressure, the particle size distribution and the particle morphology are systematically varied using full factorial experimental designs to determine the influence of these factors on the resulting physical, mechanical and thermomechanical properties.

Table 1

Particle sizes of the used and unsorted alumina raw materials.

Tabular alumina (TA)		White fused alumina (WFA)		Reactive alumina	
Particle fraction	Particle size (d_{50}) in μm	Particle fraction	Particle size (d_{50}) in μm	Raw material	Particle size (d_{50}) in μm
1–3 mm	2156.2	1–3 mm	1983.1	TE NO	2.65
0.5–1 mm	890.5	0.5–1 mm	772.2	615–10	
0.2–0.6 mm	413.3	0.1–0.5 mm	312.9	TE RG	0.76
0–0.2 mm	65.1	0–0.1 mm	52.8	4000	
		0–	17.7		
		0.045 mm			

2. Experimental

The current study involved the investigation of the factors pressing pressure (A), particle size distribution model (B) and particle morphology (C) on high purity alumina refractories. In all experiments commercial white fused (WRG, Imerys Fused Minerals Villach GmbH, Austria) or tabular alumina (T60/T64, Almatix GmbH, Germany) raw materials were used for the coarse grain fractions, while the same reactive alumina types (NABALOX, Nabaltec GmbH, Germany) were used for the fine grain fractions. The sodium and $\beta - \text{Al}_2\text{O}_3$ content were analyzed for the 0–0.2 mm and 0–0.1 mm particle fractions of tabular and white fused alumina, respectively, using a photoelectric flame photometer (M8D, Dr. Bruno Lange GmbH, Germany) and XRD (D8 Advance, Bruker Corporation, USA) together with Rietveld analysis. The sodium content of white fused alumina was 0.39 wt%, whereas tabular alumina contained slightly less sodium (0.30 wt%). For both raw materials a $\beta - \text{Al}_2\text{O}_3$ content of 3 wt% was determined. The types and particle sizes of the applied raw materials are given in Table 1.

For both alumina raw materials the investigated factors (A, B, C) were varied on two levels. Consequently, together with the factor of the used alumina raw material this resulted in three 2^2 factorial experimental designs, which are summarized together with the constant factors in Table 2. The factorial experiments were analyzed using the statistical software R [28].

To design the batches, the particle size distributions of the coarse alumina raw materials (0–0.2 mm or 0–0.1 mm, respectively, and coarser) were first determined by dynamic image analysis (Camsizer XT, Retsch Technology GmbH, Germany) according to the standard ISO 13322-2 [29,30].

For the particle analysis, the 0–0.1 mm particle fraction for WFA and 0–0.2 mm for TA, respectively, were dispersed by air pressure. The larger particle size fractions were dispersed by gravity dispersion. Moreover, the finer alumina raw materials (finer than 0–0.2 mm and 0–0.1 mm, respectively) were analyzed by laser diffraction (Mastersizer 2000, Malvern Instruments Ltd., UK).

In order to investigate the influence of the particle morphology (factor C), both alumina raw materials were then sorted regarding their particle shape using a tilted vibrating table with a rough surface. The varying shape of the particles resulted in a differing friction in contact with the surface of the vibrating table. Due to this varying friction, the particles consequently passed distinctive distances from top to bottom of the table, where the particles were collected and sorted in a row of plastic bottles.

To evaluate the effects of the particle size distribution (see Table 2, factor B), the present study compared the widely used particle packing model according to Andreasen and Andersen [31] with the recently presented packing model of Fruhstorfer and Aneziris [23] (henceforth

Download English Version:

<https://daneshyari.com/en/article/5439085>

Download Persian Version:

<https://daneshyari.com/article/5439085>

[Daneshyari.com](https://daneshyari.com)